RSC Advances

PAPER

View Article Online
View Journal | View Issue

Cite this: *RSC Adv.*, 2025, **15**, 26567

Effects of UV irradiation on the structural and optical properties of epoxy/dysprosium nanocomposite sheets for possible UV dosimetry and optoelectronic applications†

Shittu Abdullahi, *[ab] Ahmed Alshahrie,[cd] Aznan Fazli Ismail[ae] and Numan Salah *[c]

The exceptional properties of epoxy polymers are well-known because of their insulating properties, chemical resistance, and mechanical strength. Positioning them as favorable polymers compared to other polymers. But, despite these exceptional properties, epoxy materials have disadvantages, including brittleness and susceptibility to oxygen and UV light. To minimize these limitations and test the potential applications of epoxy polymers in UV sensing, we incorporated dysprosium ions (Dy^{3+}) into the epoxy matrix using a simple chemical route by employing ethanol as a suitable solvent for both materials. The sheets were characterized using multiple techniques, including SEM, XRD, Raman, and PL. Using this technique, we achieved a PL emission enhancement up to 17 times that of pure epoxy and improved UV stability. Epoxy/Dy nanocomposite sheets showed sharp PL peaks with increasing Dy^{3+} ion concentrations, besides minor shifts in the PL emission peak centers, indicating possible tuning of the optical properties of the epoxy. The epoxy sheets containing 1% of Dy^{3+} ions were further exposed to UV light for different exposure times. The PL emission intensities of the irradiated sheets exhibited changes, including variations in peak position and FWHM of the spectra, with increasing UV exposure time. Additionally, the UV sensitivity in the nanocomposite sheets was found to be significantly improved. The linearity of these sheets' response was investigated using linear regression analysis, yielding a high adjusted R^2 of greater than 98%. This high R^2 confirmed their excellent linearity response, as well as their long-term PL intensity stability, retaining over 50% of the PL intensities after one month of irradiation. Therefore, the drastic increase in PL emissions due to the presence of Dy^{3+} ions in epoxy sheets, the linearity of the response, and the long-term stability of PL intensity, in addition to the reproducibility of the signals over a long time, validate the potential of these sheets for UV sensing and other optoelectronic device applications.

Received 8th March 2025
Accepted 16th July 2025

DOI: 10.1039/d5ra01677k

rsc.li/rsc-advances

1. Introduction

Thermosetting polymers, including epoxy resins, have a wide range of applications. However, their exceptional flexibility, strength, corrosion resistance, and electrical resistance make them particularly suitable for use in adhesives, insulation, coatings, and even electronics. Furthermore, as already mentioned, epoxy resins are low in cost and their production is highly abundant, making them advantageous for use in reinforcing nano/micro composites and matrices.[1–4] Nevertheless, epoxy resins are not without their shortcomings, as they are highly susceptible to environmental exposure. Factors such as oxidation, ultraviolet light, and oxygen exposure lead to degradation of the resin's mechanical properties. Other disadvantages, such as high flammability, brittleness, and low thermal resistivity, are also disadvantages of epoxy resins.[1,2,5,6] Ironically, the UV light tends to solely affect the surface layer of the epoxy resin, which can be desired in some situations, as it allows the underlying strength of the polymer to remain intact.[5,7,8]

In the automotive, marine, construction, and even aerospace industries, lightweight yet strong mechanical parts are always essential, and that's where epoxy comes as an ideal solution. Its strength allows for use in mechanical parts, while its low weight allows for overall weight reduction.[9] Furthermore, the ability of epoxy resins to withstand extreme environmental conditions makes them perfect for use in sealants, coatings, and adhesives

[a]*Nuclear Science Program, Department of Applied Physics, Faculty of Science and Technology, Universiti Kebangsaan Malaysia, Bangi, 43600, Selangor, Malaysia*
[b]*Department of Pure and Applied Physics, Faculty of Science, Gombe State University, P.M.B. 127, Gombe, Nigeria*
[c]*Center of Nanotechnology, King Abdulaziz University, Jeddah, 21589, Saudi Arabia*
[d]*Department of Physics, King Abdulaziz University, Jeddah, 21589, Saudi Arabia*
[e]*Nuclear Technology Research Centre, Faculty of Science and Technology, Universiti Kebangsaan Malaysia, Bangi, 43600, Selangor, Malaysia*

† Electronic supplementary information (ESI) available. See DOI: https://doi.org/10.1039/d5ra01677k

as well. In the electronics domain, the use of epoxies is attributed to their low dielectric constant and high dielectric strength, which enables their application in the encapsulation of high-voltage and high-frequency LEDs and PCBs. Furthermore, epoxy resins are also used to repair and strengthen concrete structures and steel structures, as they offer anticorrosion and anti-wear benefits.[10] Additionally, owing to excellent stiffness and mechanical properties, durability, and weight, epoxy materials have become indispensable for the reinforcement of electric vehicles, airplanes, sports equipment, and wind turbine blades.[2]

The incorporation of dysprosium (Dy) ions into the epoxy matrix may enhance its optical properties, particularly in terms of photon emission and radiation response. Dysprosium is a lanthanide element that possesses a +3 oxidation state, sharp emission lines, and high luminescence efficiency under UV light.[11] Different lanthanides also emit various colors, like Tb ions emitting green, Tm ions emitting blue, Eu ions emitting red, and Sm ions emitting orange in the visible light spectrum. In contrast, others, such as Dy, Pr, Yb, Er, Ho, and Nd, primarily emit in the near-infrared region. Lanthanides emit single-wavelength light, have long luminescence lifetimes, narrow emissions, high color purity, excellent paramagnetic reaction, and significant Stokes shifts.[11–14] Because of these characteristics, they are ideal for use in laser materials, solar concentrators, organic light-emitting diodes, and UV dosimetry devices.[11,15–18]

The addition of dysprosium ions (Dy) into certain organic compounds, such as epitaxy, results in improved optical characteristics of the materials, enabling them to be used for better technology. For example, the absorption bands of Dy-doped epoxy resins are unique because they correspond to the Dy transitions and are strong photoluminescent emitters, effective in the infrared region for optoelectronic devices and UV dosimetry. Recent experiments have revealed that the addition of Dy ions, in combination with Eu ions, to a phosphor matrix ($SrAl_2O_4$) in PMMA and other polymers significantly increases the duration of phosphorescent afterglow. This change enhances material stability under UV light, making it more suitable for solid-state lighting applications. Moreover, in the form of epoxy, Dy ions have proven to retain intrinsic luminescent properties when sealed in polymer matrices, which indicates the ability to develop high-efficiency and long-lasting UV-responsive materials.[19–21] Therefore, incorporating Dy ions into epoxy could enhance its properties by making it more responsive to UV radiation, thereby enhancing its effectiveness as a UV dosimetry device. Polymers, including epoxy, are typically damaged by UV light due to chain scission, resulting in a reduction in molecular weight and changes in mechanical properties such as strength.[22] The introduction of Dy ions within an epoxy matrix could alleviate such effects by manipulating light emission characteristics and thus potentially mark an improvement on traditional UV dosimeters. It is important to note that there are no markers in the literature on the effects of UV irradiation on Dy-containing epoxy sheets used for radiation dosimetry. That is why it is important and interesting to study how UV radiation affects the chemical and optical properties of Dy-doped epoxy resins.

To the best of our knowledge, this study is the first to explore the combined structural and optical effects of UV irradiation on epoxy sheets doped with Dy^{3+} ions. We demonstrate a significant enhancement in photoluminescence up to 17 times that of pure epoxy, as well as tunable emission properties and excellent linear response under UV exposure. These findings introduce a promising new class of low-cost, UV-sensitive nanocomposites with potential applications in optoelectronics and radiation dosimetry, areas where such polymer-based systems remain underexplored.

2. Materials and methods

2.1 Materials

The following materials were used in this research: glass slides, DyCl3 powder, ethanol (EtOH), epoxy resin, and hardener (REPCON IR), as well as pipettes. The epoxy resin and hardener were supplied by Construction Materials Chemical Industries (CMCI), Dammam, Saudi Arabia, which has a low viscosity of its products. DyCl3 was purchased from Sigma Aldrich with a purity of more than 98%. The ethanol used in the experiments was also purchased from Sigma Aldrich. The instruments used in this study include a water bath sonication machine (BRANSON ULTRASONICS SERIES 3510R-DTH), with an output of 100 W and an operating frequency of 42 kHz ± 6%, which is from the USA; an electric furnace; and an AREC heating magnetic stirrer (VELP SCIENTIFIC) with a digital display for timing and temperature control.

2.2 Method

To prepare the epoxy sheets, a 60 minutes degassing process was used to remove air from a 20 mL epoxy resin and 10 mL ethanol mixture, resulting in the creation of the epoxy sheets. The mixture received 10 mL of hardener after degassing and was stirred for 10 minutes. The solution required for this process was poured onto glass slides that underwent a cleaning process using deionized water, followed by methanol and acetone. To incorporate Dy ions into the epoxy matrix, DyCl3 was dissolved in 10 mL of ethanol and subjected to sonication for 1 hour. We kept the solution stirred with a magnetic stirrer for 2 hours. We mixed the hardener with the epoxy after one hour of degassing and manually stirred for 10 minutes. We then applied the solution to glass slides by drop casting. We left the nanocomposite sheets to dry at room temperature for 24 hours before placing them in a 70 °C furnace for 5 hours, as shown in Fig. 1. The prepared nanocomposite sheets were then stored in the laboratory before the irradiation process. The nanocomposite sheets were prepared containing varying weight percent (wt%) of Dy using $DyCl_3$ corresponding to the total mass of epoxy resin and hardener. The weight percents of $DyCl_3$ considered are 0.1 wt%, 0.5 wt% and 1 wt%, respectively. Therefore, for simplicity, these percentages are written in the manuscript as 0.1%, 0.5%, and 1%, respectively. Furthermore, to reduce the hygroscopic effect of $DyCl_3$ and minimize the possibility of water absorption or hydrolysis during preparation, the $DyCl_3$ powder was dissolved in ethanol immediately after

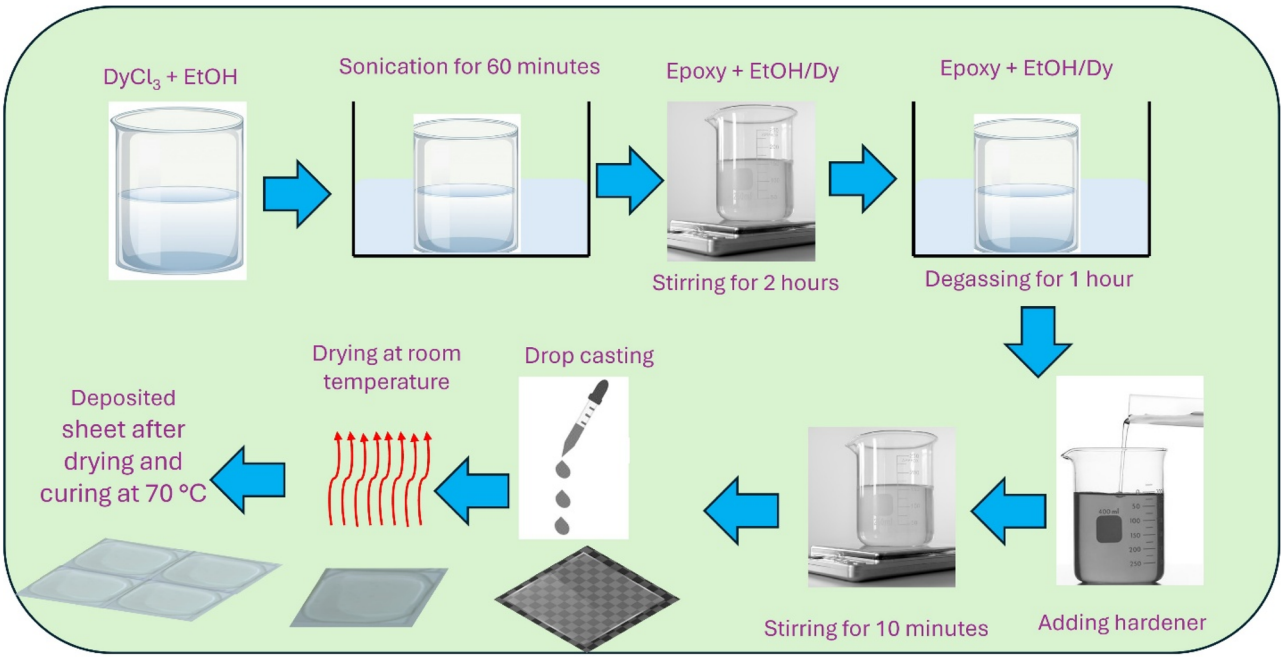

Fig. 1 Preparation of epoxy/Dy nanocomposite sheet.

opening. The solution was then sonicated and stirred in a covered container to limit exposure to air and moisture. We also degassed the epoxy–ethanol mixture before adding the hardener, which helped remove any trapped air or residual moisture. The curing temperature of 70 °C was deliberately kept moderate to avoid thermal decomposition or formation of DyOCl. Although we did not specifically analyze for residual water or hydrolysis products, the preparation steps were carefully controlled to ensure uniform dispersion of Dy ions and reduce any influence on the optical properties of the composites.

2.3 UV irradiation of nanocomposite sheets

The SPDI UV Exposure Lab Chamber model 800.977.7292 delivered high-intensity UV light to nanocomposite sheets made from pure epoxy and epoxy mixed with Dy. The sheets were positioned 10 cm from a 160 W light source with an irradiance of 127 mW cm^{-2} for testing. Irradiation was conducted for different exposure durations, with the samples receiving 1, 2, 5, 10, and 20 minutes of UV radiation treatment.

2.4 Characterization of nanocomposite sheets

We studied both pure epoxy sheets and their nanocomposite variations before and after UV irradiation through multiple test methods. A JSM-7500 JEOL system, operating at 10.0 kV, analyzed the surface details of our samples using Scanning Electron Microscopy (SEM). A DXR micro-Raman system with 532 nm laser excitation and a 10 mW source power was used to examine the material vibrations through Raman Spectroscopy. An X-ray diffractometer, Rigaku Ultima-IV, originally from Japan, was used to determine the crystalline structure of the nanocomposite sheets. The setup was equipped with a parallel beam and a thin-film attachment. To run the system, a current of 30 mA and a voltage of 40 kV were required. The period was 0.05°, and 2θ was in the range of 10° to 80°. The method also used Cu Kα as a source with a wavelength of 1.5418 Å, a step time of 2 seconds, and an incidence radiation angle of 1°. The photoluminescence (PL) spectrum was investigated using an RF-5301PC Spectrofluorophotometer (Shimadzu, Japan), with an emission wavelength range of 400 to 700 nm and an excitation wavelength of 380 nm. Moreover, measurements were taken *via* fast scanning speed mode with identical excitation and emission slit widths of 5 nm to ensure high-quality and accurate emission intensities.

3. Results and discussion

3.1 Surface morphology of the pristine epoxy and epoxy/Dy nanocomposite sheets

Fig. 2(a) and (b) show the surface morphology of the sheet at different magnifications. The surfaces illuminated in these images at the specific magnification appeared to be pure and even. However, when Dy ions were introduced into the epoxy sheet at varying concentrations, there was a big difference in the surface morphology, as seen in Fig. 3. Specifically, Fig. 3(ai) and (aii) present the surface morphology of the epoxy sheet solely containing 0.1% Dy ions. These images demonstrate a characteristic pattern composed of many micro-sized particles. Fig. 3(bi) and 3(bii) show different patterns of micro-sized particles for the sheet with 0.5% Dy ions. In this case, we notice that they are more than in the 0.1% Dy sample. Finally, Fig. 3(ci) and 3(cii) are the only images that show the surface morphology of the epoxy sheet with 1% Dy ions, which appears completely different, with both the size and distribution of micro-sized particles being unique.

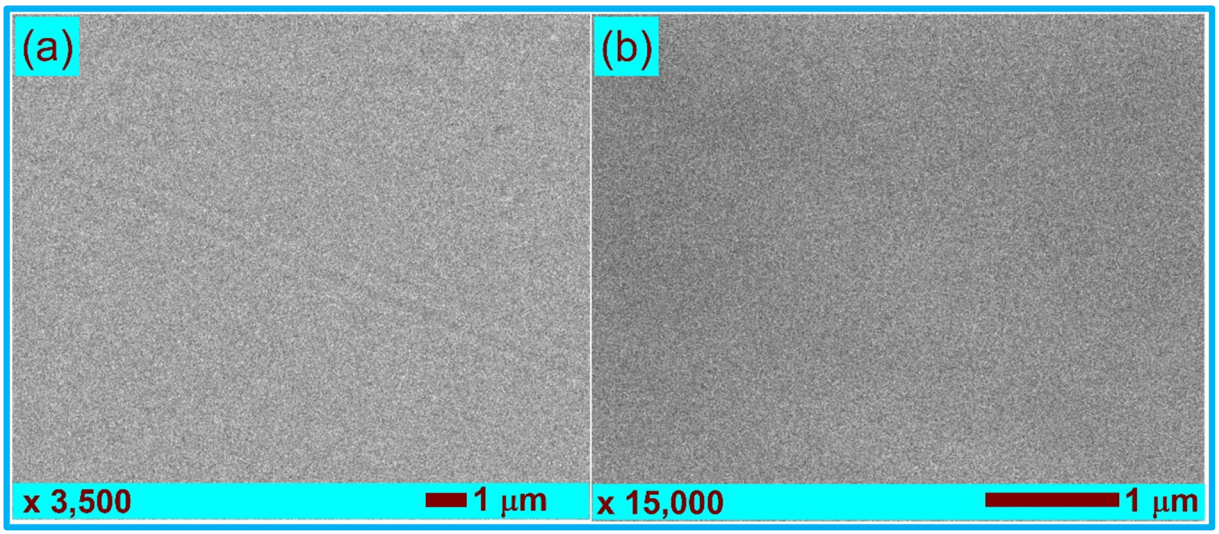

Fig. 2 (a) and (b) SEM images of epoxy sheets at different magnifications.

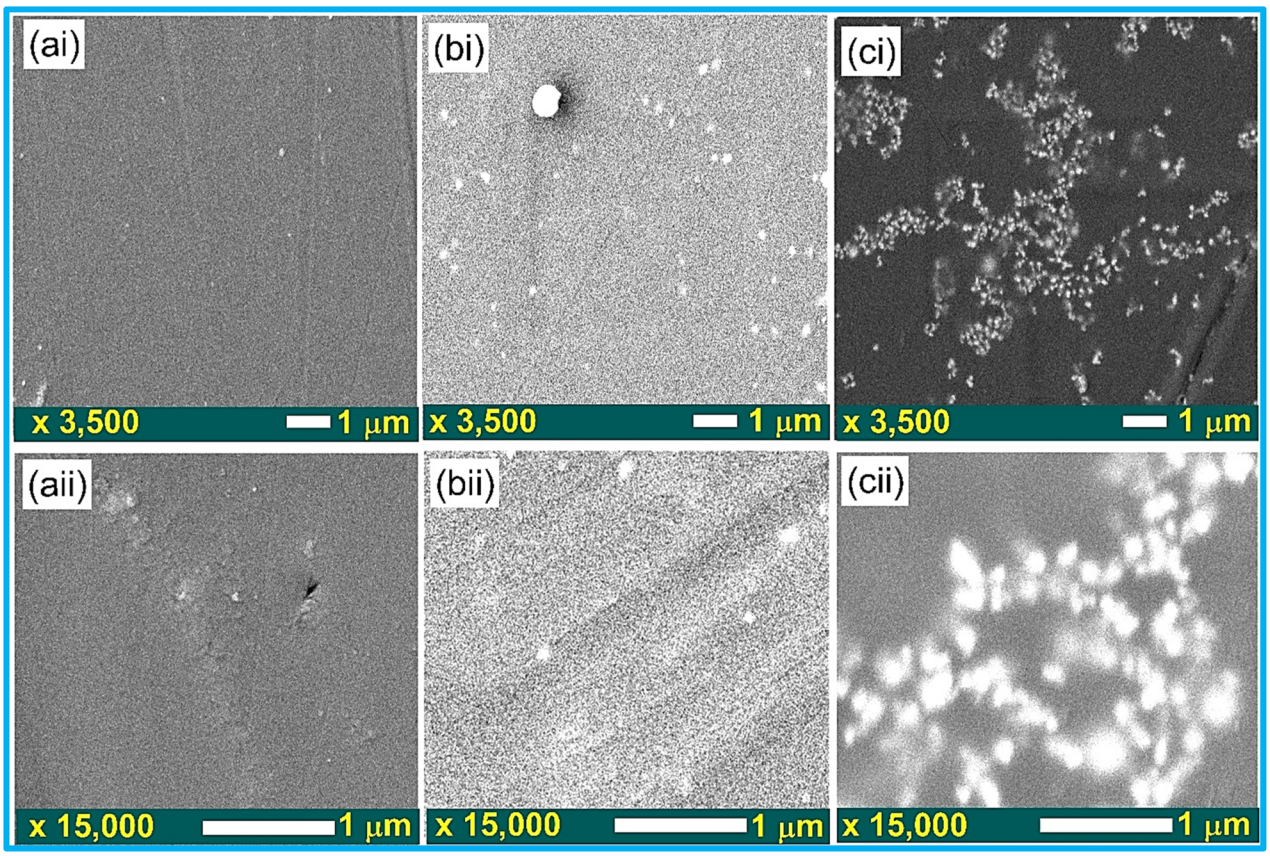

Fig. 3 SEM images of epoxy sheets containing different concentrations of Dy ions: (ai) and (aii) 0.1% Dy, (bi) and (bii) 0.5% Dy, and (ci) and (cii) 1% Dy.

The micro-sized particles seen on the nanocomposite sheets were within different specified size ranges: 0.1% Dy ions were sized in the range of 108–476 nm, 0.5% Dy ions were sized in the range of 99–352 nm, and 1% Dy ions were sized down to 81–244 nm. Also, the mean particle sizes of respective sheets were determined to be 229 ± 99 nm, 207 ± 78 nm, and 167 ± 40 nm. It should be said that as the concentration of Dy ions in the nanocomposite is increased, the particle size is slightly reduced. This observation implies that the rise in Dy ion concentration is the cause of a more homogenized and larger size distribution of particles on the surface of the epoxy sheet. Although some aggregation and uneven dispersion are

observed, especially at lower Dy content, these effects appear to diminish as the Dy concentration increases, leading to better distribution and reduced particle size. This improved uniformity may positively influence the material's functional properties. There are no marked differences in either the length of the SEM images of the epoxy sheet and epoxy/Dy nanocomposite under UV irradiation or surface appearance and structural integrity in comparison to the sheets that were not irradiated. This means that the UV exposure time for both the epoxy and the nanocomposite sheet has no significant impact on them. Nevertheless, despite the absence of any variations in the SEM images, it is essential to emphasize that UV irradiation did cause the molecular structure and PL properties of the epoxies to change at a molecular level. These minute but significant shifts will be further discussed in the following sections of the results.

3.2 X-ray diffraction pattern of pristine epoxy and epoxy/Dy nanocomposite sheets

XRD study highlights the significant impact of Dy ions on the crystalline structural properties of epoxy-based nanocomposites, even at low dopant concentrations. The diffraction patterns of a pure epoxy sheet and Dy-doped composites (0.1%, 0.5%, and 1% Dy) were recorded at room temperature and are presented in Fig. 4. The pure epoxy sheet exhibited an amorphous nature, as indicated by the absence of sharp diffraction peaks. It confirms earlier observations by previous authors who ascribed the amorphous nature of the epoxy to its molecular structure, hence, after curing, leading to the formation of permanent and glassy structures with no crystallization behavior due to the three-dimensional network formed between the monomer and hardener.[23] This was not the case for nanocomposites with varying percentages of 0.1%, 0.5%, and 1% Dy, which showed some prominent diffraction peaks indexed using the JCPDS card number 22-0612, matching earlier work done by.[24–27] These peaks correspond to the Dy cubic phase. They are even present at low levels of Dy, indicating that Dy ions tend to form crystalline phases inside the epoxy matrix, in agreement with similar studies performed on polymer matrices.[19–21] Notably, three diffraction peaks (411), (440), and (444) appear in both the 0.5% and 1% Dy-doped samples but are absent in the 0.1% Dy-doped sample and the pristine epoxy, indicating a threshold concentration for the formation of these specific Dy-rich crystalline planes. Additionally, two other diffraction peaks (400) and (631) are observed exclusively in the 1% Dy-doped sample. These peaks do not appear in the lower Dy concentrations, suggesting that their formation requires a higher Dy ion concentration to promote sufficient crystallization along those planes. This progression of peak appearance with increasing Dy content strongly supports a concentration-dependent nucleation and growth mechanism, where higher Dy levels facilitate the formation of more defined and diverse crystalline orientations within the nanocomposite.

The relative intensity of specific reflections also varies with Dy concentration. For instance, the (431) peak reaches maximum intensity at 0.5% Dy but diminishes slightly at 1%, while the (622) and (611) reflections exhibit a different trend, reduced intensity at 0.5% Dy, which then recovers at 1%. This non-monotonic behavior may be attributed to the dual role of Dy ions: at intermediate concentrations, they may disrupt local ordering, whereas at higher concentrations, they facilitate more extensive crystalline clustering. Note, these additional peaks are consistent with those indexed in the cubic Dy_2O_3 phase (JCPDS 22-0612), confirming the crystallographic assignment.

Similar observations have been reported in both polymer-based and oxide systems, particularly involving lanthanides. For example, TiO_2 doped with different concentrations of Dy_2O_3 exhibited a phase transition from rutile to a Dy-rich secondary phase that only emerged at higher dopant levels. This transition was marked by the appearance of new diffraction peaks that were not present in the pristine TiO_2 ceramics, indicating the formation of distinct crystalline domains.[28] In another study, Y_2O_3 nanoparticles embedded in a polypyrrole (PPy) matrix showed additional diffraction peaks at the (440) and (622) planes only after doping. In contrast, some existing peaks disappeared, further supporting the role of dopants in modifying crystallinity.[29] Similarly, Dy_2O_3-doped TiO_2 nanoflowers revealed new peaks around 27.3° and 38.8°, which were absent in the undoped material and became more prominent with increasing Dy content, highlighting the formation of secondary crystalline phases.[30] PEI-capped Dy_2O_3 nanoparticles also displayed distinct peaks indexed to the cubic Dy_2O_3 phase, which were not observed in the amorphous polymer matrix, confirming that these peaks originate from the dopant crystallites rather than the host matrix.[31] Likewise, the study by Moreno *et al.* (2023) on the green synthesis of Dy_2O_3 nanomaterials reported characteristic peaks corresponding to the cubic phase, lending further support to the emergence of well-defined Dy-rich crystalline structures, especially at higher doping levels.[32] Therefore, the additional XRD peaks observed in our epoxy/Dy nanocomposite sheets are consistent with these earlier findings. Although new peaks emerge with increasing Dy content, the overall pattern remains indexed to the cubic Dy_2O_3 phase. This suggests that while the dopant enhances crystallinity and promotes the development of specific orientations, the fundamental crystalline structure is retained within the composite.

Most diffraction peaks exhibit a shift toward higher diffraction angles (2θ) with increasing Dy concentration, indicating lattice contraction or strain resulting from Dy incorporation. Peak broadening is also observed with higher Dy content, consistent with a reduction in crystallite size. The average crystallite sizes calculated using the Debye–Scherrer equation were 23.57 ± 4.98 nm for 0.1% Dy, 14.82 ± 0.65 nm for 0.5% Dy, and 13.60 ± 1.37 nm for 1% Dy. This decrease in crystallite size with increasing Dy content aligns well with the nanoparticle sizes observed in the SEM images, supporting the overall trend. The term "crystallinity" here refers to the appearance and growth of crystalline Dy_2O_3 phases within the amorphous epoxy matrix. We do not suggest that the epoxy itself becomes crystalline, but instead that the addition of Dy introduces well-defined crystalline regions that influence the structural and optical properties of the composite. This behavior is consistent with previous findings on Dy-doped materials, where such dopants enhance both structural features and functionalities, such as luminescence and UV sensitivity.[19,21]

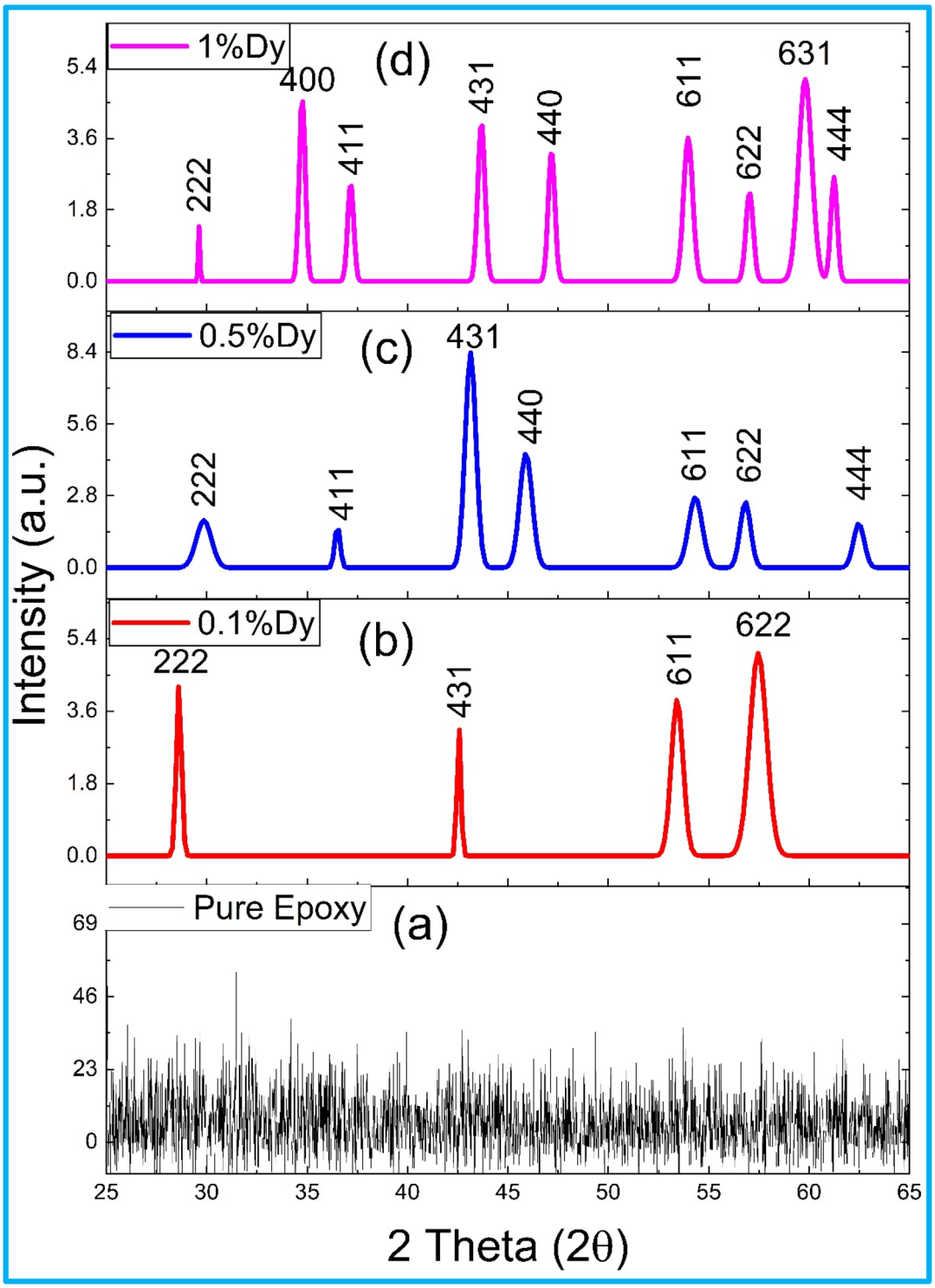

Fig. 4 XRD patterns of the pure epoxy sheet (a), and its nanocomposite sheets containing various concentrations of Dy ions: 0.1% Dy (b), 0.5% Dy (c), and 1% Dy (d).

3.3 Molecular fingerprint of the pristine epoxy and epoxy/Dy nanocomposite sheets

Raman analysis investigates the molecular structure and chemical composition of the epoxy and epoxy/Dy nanocomposite sheets. Fig. 5(a) presents the Raman spectra of both samples, showing different vibrational modes corresponding to the various molecular parts of the epoxy and epoxy/Dy nanocomposite sheets. In the Raman spectrum of epoxy, peaks at 637, 824, 1113, 1184, and 1235 cm^{-1} are assigned to epoxy ether bonds, C–O–C, and C–C bonds within its backbone,[33–36] and aromatic stretching mode at 732 cm^{-1}.[33,37] The peaks at 1298 and 1433 cm^{-1} indicate asymmetric aryl alkyl ether vibrational mode (C–O–C) and C=C linkages within the aromatic

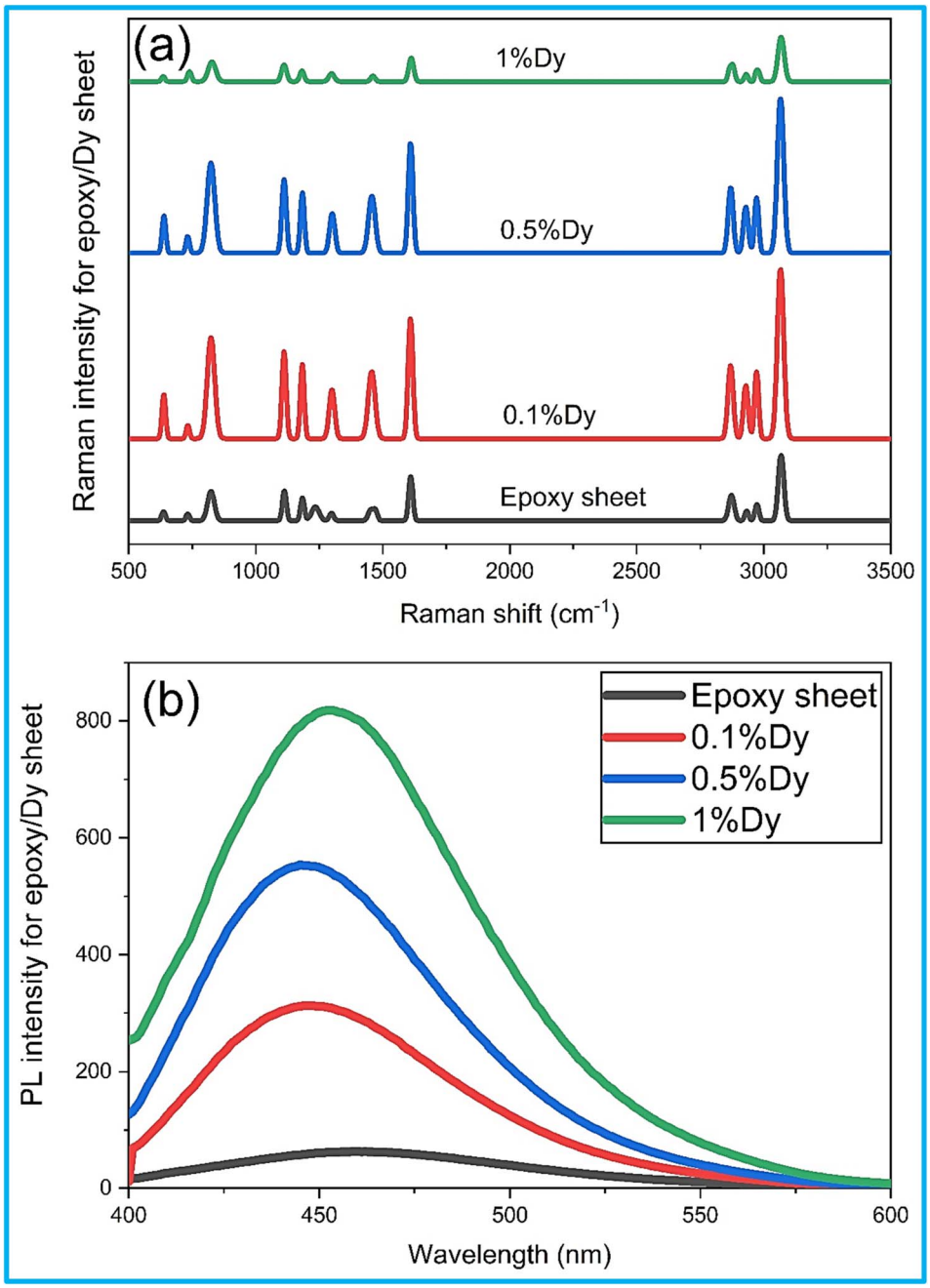

Fig. 5 Characterization of pristine epoxy sheets containing different concentrations of Dy ions: (a) Raman spectra of epoxy/Dy sheets and (b) PL emission spectra of epoxy/Dy sheets.

structure.[33,35] The peaks at 1471, 2873, 2933, and 2973 cm^{-1} correspond to the symmetric and asymmetric stretching modes of CH_2 and CH_3 units, whereas the peak at 1610 cm^{-1} corresponds to the ring stretching mode.[34,38,39] The peak at 3068 cm^{-1} is due to the aromatic C–H stretching mode.[40] In the case of the epoxy/Dy nanocomposite, the Raman peaks at 534 cm^{-1} and 744 cm^{-1} have been assigned to Dy–O and Dy–Cl stretching modes,[24] respectively.

However, these peaks were also observed for the pure epoxy sample, and thus, a possible spectral overlap cannot be excluded. To clarify the peak assignment, energy-dispersive X-ray spectroscopy (EDS) was performed using the SEM system. The EDS analysis confirmed that the pure epoxy consists of carbon and oxygen, while the nanocomposite also contains Dy in addition to carbon and oxygen. Chlorine (Cl) was not detected in either sample. Consequently, it was unequivocally ascertained that the aromatic stretching mode- and not Dy–Cl, as mentioned by some works in the literature corresponds to a Raman peak at 732 cm^{-1}.[24]

Although the Raman spectral shifts are relatively minimal, the variation in Raman peak intensities and the full width at half maximum (FWHM) as a function of Dy ion concentration reveals key insights into defect formation and the structural perturbations introduced by Dy doping. In this respect, the

Raman intensities of the epoxy/Dy nanocomposite were increased at Dy ion concentrations of 0.1 and 0.5%. In comparison, the decrease was considerable at 1% Dy ions, possibly due to defect formation resulting from the excess Dy ions. Such intensity modulation is often indicative of changes in local order and symmetry, even in the absence of significant shifts in peak position. Besides, it seems that the FWHM of the Raman spectra is less sensitive to the Dy ions concentration. In this respect, the values of FWHM for nanocomposite sheets are 21.23, 21.81, and 22.64 cm^{-1} for 0.1%, 0.5%, and 1% Dy ions, respectively. With an increase in the concentration of Dy ions, the FWHM value increases gradually; this may be due to the defects created by the excess amount of Dy ions in the nanocomposites. Additionally, the slight broadening observed with increasing Dy content may reflect enhanced phonon scattering due to increased structural disorder.[41,42]

Importantly, the novelty of this analysis lies in our integrative approach that combines Raman spectroscopy with EDS and XRD techniques to confirm the presence of Dy, clarify ambiguous peak assignments, and detect subtle structural modifications in the polymer matrix. To our knowledge, this synergistic use of vibrational and compositional analysis to assess defect-related changes in epoxy/Dy nanocomposites has not been previously reported.

3.4 PL emission spectra of the pristine epoxy and epoxy/Dy nanocomposite sheets

Fig. 5(b) shows the PL emission spectra of the pristine epoxy sheets and the sheets of the epoxy/Dy nanocomposite. The PL spectrum for the pristine epoxy sheet is a broad peak centered at 459 nm with a FWHM of 98 nm. In contrast, Dy-doped epoxy sheets showed emission peaks at the center of 445 nm, 446 nm, and 453 nm for Dy ion concentrations of 0.1%, 0.5%, and 1%, respectively, with FWHM values of approximately 76 nm, 77 nm, and 88 nm. The addition of Dy ions significantly affects the emission profile of epoxy due to the change in intensity, peak position, and FWHM. It can be observed that as the Dy ion concentration increases, the PL emission intensity increases considerably. For example, whereas the intensity of the pristine epoxy sheet is about 63, the addition of 0.1% Dy increases the intensity by a factor of about 5, increasing further to nearly 11 and 17 times the initial intensity for 0.5% and 1% Dy, respectively. This indicates an increased area under the emission spectrum with a higher Dy concentration, which represents the enhanced light emission. Most interestingly, FWHM decreases from 98 nm for the pure epoxy sheet to a value of 76 nm at 0.1% Dy, which depicts the reduction of emission broadening. Upon further increasing the Dy concentration, FWHM slightly broadened to 88 nm for 1% Dy, which, even then, was not as wide as the FWHM of the pure epoxy sample. This narrowing reflection would suggest the development of defects or carrier transfer inside the epoxy matrix, which results in increased PL intensities.[43–46]

Furthermore, the red shift in emission from 459 nm for pure epoxy to 445–446 nm at Dy concentrations has been observed, indicating that Dy ion incorporation allows for tuning of light–emission properties. The shifting in the PL peak position may also be related to morphological changes; SEM images also showed that, although the surface of pristine epoxy was smooth, Dy-doped sheets showed uniform distributions of particles in the sheets. This would mean partial interaction of epoxy with the Dy ions. In most inorganic compounds, Dy ions usually exhibit two important emission bands at about 380 nm (blue-violet) and 575 nm (yellow), ascribed to transitions within Dy^{3+} (namely, $^4I_{15/2} \rightarrow {}^6H_{9/2}$ and $^4F_{9/2} \rightarrow {}^6H_{13/2}$). These bands may be shifted or broadened in organic hosts, such as epoxy or PMMA, due to interactions with the organic matrix. These organic matrices have different dielectric properties and more complicated bonding environments than inorganics, which changes the local symmetry and electronic surroundings of Dy ions, modifying their emission characteristics.[19,20]

The band gap and excitation wavelength of Dy-doped organic nanocomposites can also shift. Since organic hosts, such as epoxy, usually have a larger band gap compared to inorganics, the excitation energy may increase, and energy transfer pathways to Dy ions may change. These effects can reduce Dy excitation efficiency or shift emission peaks since the organic ligands modify Dy's luminescence properties. For instance, Dy-doped epoxy systems show different PL features compared with inorganic ones, and in most cases, a change in the excitation wavelength is needed to get the best luminescent performance.[20,21] Finally, the nature of the host matrix has often been identified as decisive in defining the optical features of Dy-doped nanocomposites. The host matrix acts on the luminescence efficiency, on the emission wavelength, and therefore on the overall resulting optical output. Additionally, the observed enhancement in PL intensity is attributed to the luminescent nature of Dy^{3+} ions, which act as efficient activators by introducing new radiative recombination centers within the epoxy matrix. The interaction between Dy ions and the host modifies the local environment and promotes energy transfer from the host to the Dy centers, leading to intensified emission.[43,44]

3.5 Effects of UV irradiation on epoxy composite sheets

3.5.1 Effects of UV exposure on Raman spectra of epoxy and epoxy/Dy nanocomposite sheets. In this study, the changes in molecular structure and chemical composition of a sheet of neat epoxy and Dy ion nanocomposites (1% Dy) were investigated after exposure to UV-light irradiation, and their Raman spectra were compared using Raman spectroscopy. Fig. 6(a) shows the variation of the Raman spectra of the epoxy sheet after UV treatment, which included a shift in the spectrum and the disappearance of some peaks. As observed from this figure, with an increase in the time of exposure to UV, there is a systematic increase in Raman intensity, indicating that more prolonged UV exposure would introduce larger molecular changes. Thus, the disappearance of Raman peaks at 637 cm^{-1}, 1235 cm^{-1}, and 2933 cm^{-1} corresponding to the breaking of epoxy ethers with bonds involving C–O–C, C–C, and C–H has vanished after 20 minutes, which depicts the breaking of the bonds mentioned above.[33–35]

The Dy^{3+} ions containing a nanocomposite sheet after exposure to UV light were taken for a Raman spectrum, shown

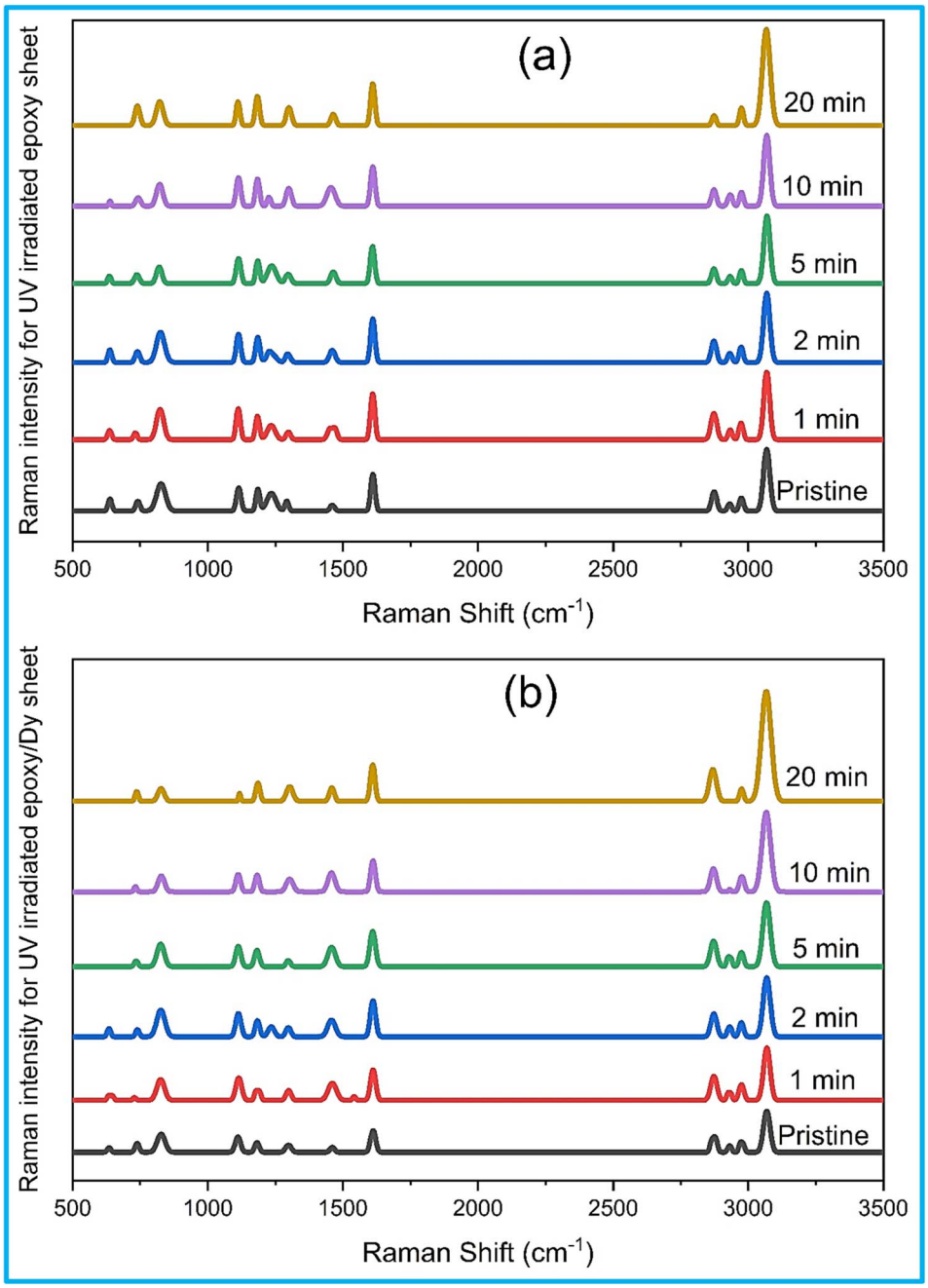

Fig. 6 Raman spectra of UV irradiated sheets containing Dy ions: (a) epoxy sheets and (b) epoxy/Dy sheets.

in Fig. 6(b), which evidences the increase in Raman intensity due to an increased number of –OH radicals upon increased time exposure. By and large, the peak at 637 cm^{-1} is found depleted within an irradiation period of the teensy and remains completely until it reaches 20 min. Analogous to its pure epoxy nanosheets, peak 2933 cm^{-1} had disappeared entirely at and beyond 20 min duration of UV irradiation. The implications of the observations are explanations of how the integrity of the UV light affects epoxy matrices, especially how Dy ions can influence the same induced changes. Generally, the changes of the Raman spectrum between an irradiated and pristine epoxy sheet imply a change in the molecular structure of such material in response to UV exposure. The Raman spectrum provides information on the vibrational modes of the material's molecules; thus, it follows that when the peaks shift in position, increase in intensity, or vanish, some action may be taking place with the chemical bonds in the material.

These can be the possible implications for disappearing Raman peaks in the case of both irradiated epoxy sheets and nanocomposite sheets with Dy ions: (i) Raman peaks corresponding to disappearing bands correspond to certain molecular bonds like C–O–C-epoxy ether bonds, C–C, and C–H. Disappearing indicates that these are breaking down. The breakdown can thus indicate the chemical degradation of

epoxy. (ii) The molecular bonds that are affected by UV exposure contribute not only to the chemical composition but also to the material's mechanical properties. The degradation of these bonds could therefore lead to reduced strength, elasticity, and resilience in the epoxy and in the nanocomposite material. (iii) In cases where materials are exposed to the outdoors or even to UV in applications, the stability of their molecular structure is highly relevant. Changes in the Raman spectra recorded may correspond to poorer wear resistance, durability, and longevity performances. (iv) The presence of Dy ions in the nanocomposite might indicate some interaction with UV light that may interfere with the rate of degradation. For example, the 637 cm^{-1} peak completely disappeared after only 5 min of UV exposure in the nanocomposite sheet containing Dy ions, which may suggest that the presence of these ions accelerated the degradation process.

3.5.2 Effects of UV exposure on PL emission spectra of epoxy and epoxy/Dy nanocomposite sheets. This study investigates the impact of UV irradiation on PL emission from an epoxy sheet and its nanocomposite doped with 1% Dy ions. PL emission spectra for the pristine sheets, as well as those after UV irradiation, are presented in Fig. 7, obtained using a PL

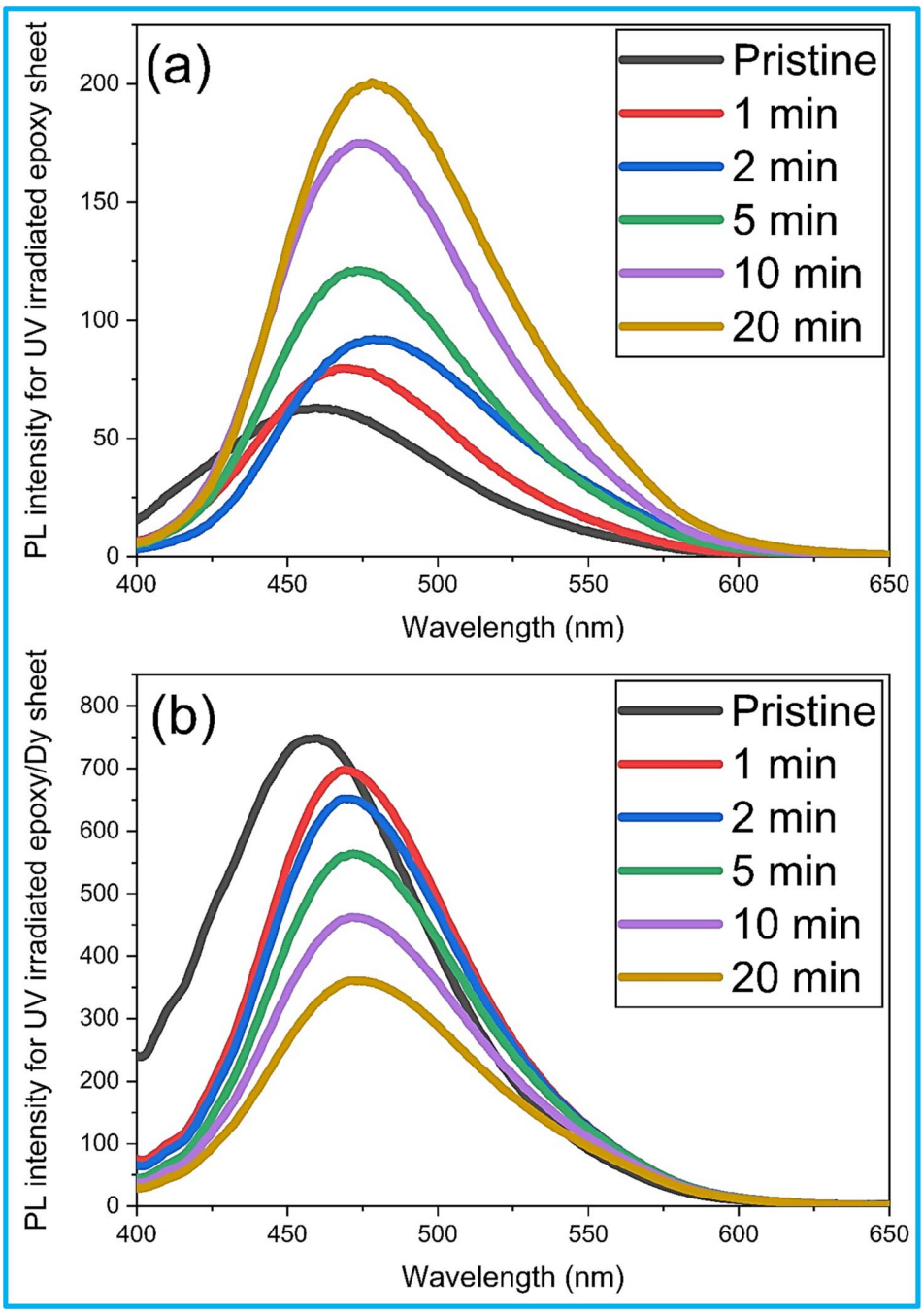

Fig. 7 PL emission spectra of UV irradiated sheets containing Dy ions: (a) epoxy sheets and (b) epoxy/Dy sheets.

spectrophotometer. Specifically, Fig. 7(a) shows the variations of PL spectra of the pristine epoxy sheet before and after exposure to UV light. Amongst the changes observed due to UV exposure are spectral shifting, FWHM variation, and PL emission intensity variation. The emission peak of the pristine PL emission was at 459 nm and shifted to 481 nm after 2 min UV light exposure. After 20 min of UV exposure, a PL position shifted to 476 nm was then produced. FWHMs were also found to decrease with time. Still, the intensity *vs.* time and its related integrated area over the PL-spectra increased with increasing UV irradiation exposure time in systems. Fig. 7(b): in an epoxy/Dy nanocomposite, the PL spectra change in much the same way, while PL position continuously shifts with changing exposure time in UV light, varying systematically from 453 to 472 nm in 20 min UV irradiation; FWHM declines correspondingly in epoxy/Dy sheets as time prolongs. Simultaneously, the PL intensities and the integrated area of the PL emission spectrum decreased systematically with increasing irradiation time.

The light emission tuning can be induced by irradiating epoxy sheets and epoxy/Dy nanocomposite sheets with UV light for different durations. Both epoxy and epoxy/Dy sheets demonstrated a significant green shift in the center position of their emission intensities, with wavelength shifts of approximately 17 nm and 19 nm, respectively. These shifts indicate the strong potential for tuning light emission through UV exposure. UV irradiation also sharpened the PL emission spectrum of the epoxy sheet, as evidenced by the systematic decrease in FWHM values over time. This increase in sharpness also favorably enhanced PL emission intensities and the integrated area of the PL spectrum of the epoxy sheets. In contrast, the slight variations in FWHM of the epoxy/Dy sheet may have a significant effect on the PL intensities and the integrated area of the PL spectrum, inducing a systematic decrease in both. Given this, the results of this study provide insight into the effects of UV light exposure on the PL properties of epoxy sheets and epoxy nanocomposites containing 1% Dy ions. The changes in PL spectra, such as shifts in emission peaks, changes in FWHM, and variations in intensity, thus obtained, become highly relevant for various applications of this material in optoelectronic devices and radiation dosimetry.

In other words, due to UV exposure, the PL emission spectrum of the epoxy sheets shifted from 459 nm to 481 nm after 2 minutes and slightly to 476 nm after 20 min, indicating that some dynamic interaction of UV light with the epoxy matrix is present, probably involving photoinduced chemical modifications or structural rearrangements within the material. This initial redshift, followed by a slight blueshift, can be explained by the formation of new emissive states during early exposure, which gradually reorganize or degrade under prolonged irradiation. In contrast, the epoxy/Dy nanocomposite shows a steadier and continuous redshift throughout the UV exposure period. This suggests that the Dy ions may help stabilize the emission environment and prevent significant structural changes, leading to a more uniform spectral shift over time. The summary of the PL peak positions and FWHM of the pure epoxy sheet and its nanocomposite sheet containing 1% Dy ions is presented in Table 1:

Table 1 UV irradiation time, PL peak position, and FWHM of pure epoxy and epoxy nanocomposite containing 1% Dy ions

Irradiation time (min)	PL peak position (nm)	FWHM (nm)
Pure epoxy sheet		
0	459 ± 3	97.5 ± 1.5
1	469 ± 8	84.6 ± 2.4
2	481 ± 12	89.3 ± 2.1
5	473 ± 5	83.9 ± 1.7
10	474 ± 7	82.4 ± 1.8
20	476 ± 4	84.1 ± 0.8
Epoxy/Dy nanocomposite sheet		
0	453 ± 5	87.5 ± 1.1
1	467 ± 10	79.8 ± 1.7
2	469 ± 6	79.4 ± 1.5
5	470 ± 3	78.9 ± 1.3
10	471 ± 4	80.1 ± 1.2
20	472 ± 7	81.5 ± 1.3

Correspondingly, in epoxy/Dy nanocomposite sheets, the shift was observed to vary from 453 nm in the pristine state to 472 nm after 20 min of UV irradiation. Such a shift, once again, highlights the impact of Dy ions on the modulation of emission features under UV-irradiated conditions. Unlike the epoxy sheets, only slight decreases in FWHM of the epoxy/Dy nanocomposites were recorded, suggesting that Dy ions stabilize the emission properties. Systematic reductions in both PL intensities and the integrated area of the PL spectrum for UV exposure times suggest a probable quenching effect or degradation of the luminescent centers as time progresses. This recorded behavior can be attributed to the interaction of UV light with the Dy ions and the resulting energy transfer processes *via* non-radiative routes or the formation of non-emissive groups.

After UV irradiation, the different behaviors of the epoxy and epoxy/Dy nanocomposite sheets underline their potential applications in various fields. The possibility of tuning the emission wavelength through UV exposure, as demonstrated by the green shifts in both materials, enables their application in optoelectronic devices where specific emission characteristics are required. The enhanced sharpness and intensity of the PL emissions in epoxy sheets suggest their suitability for applications demanding high emission efficiency and spectral purity. Conversely, the controlled reduction in PL intensity and integrated area obtained in the present epoxy/Dy nanocomposites may be helpful in applications requiring a temporary decrease in emission, such as dosimetry. The PL intensities would show a systematic decrease with increased exposure, providing a reliable measure of the radiation dose for accurate monitoring and control.

3.5.3 Linear regression analysis of the Raman and PL intensity variations in UV irradiated epoxy and epoxy/Dy nanocomposite sheets. Linear regression is a statistical method used in estimating the linear relationship between two variables. In this paper, linear regression is used to study the

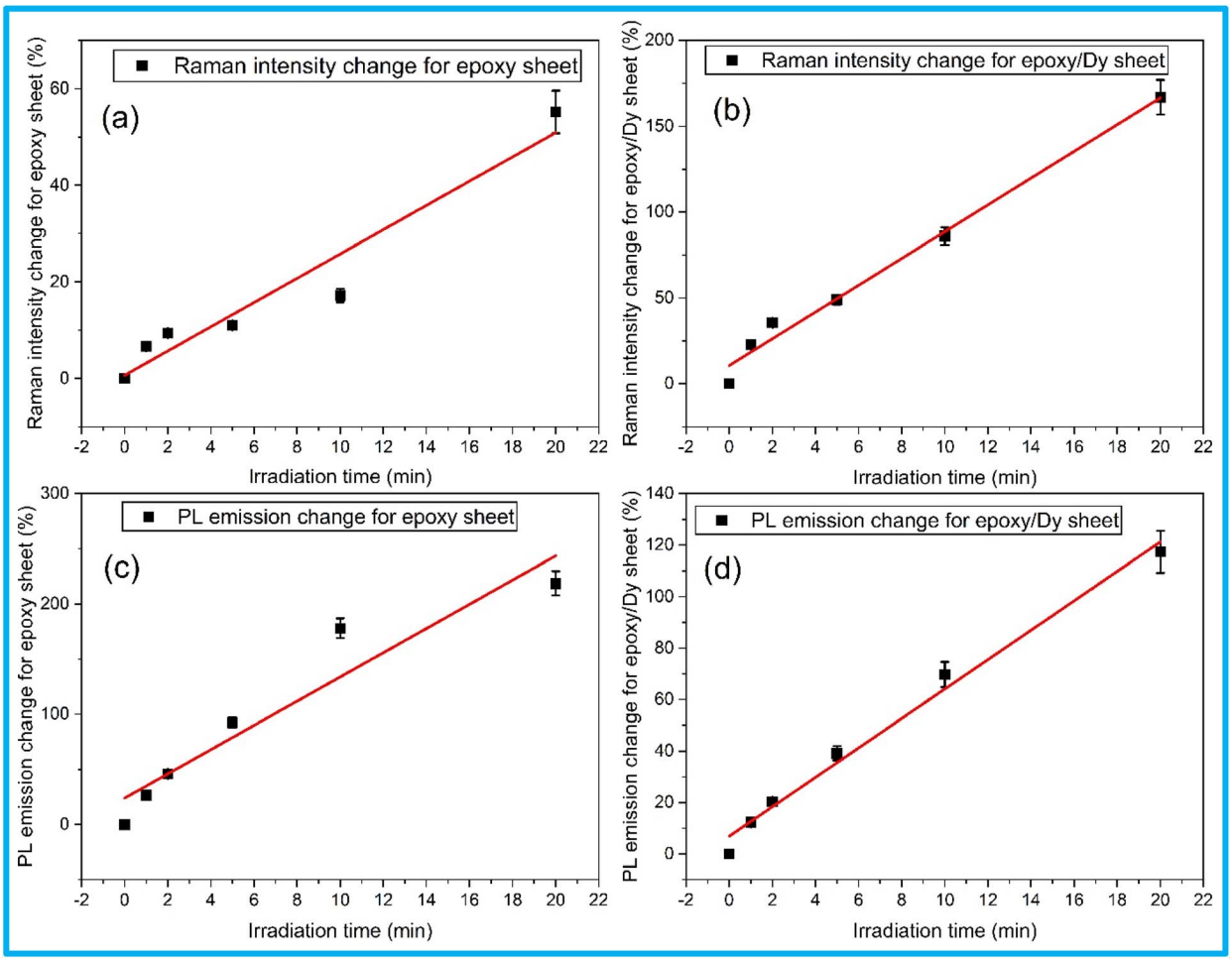

Fig. 8 Percentage induced changes by UV irradiation in Raman intensities: (a) epoxy sheet, (b) epoxy/Dy sheet, and PL emission intensities change: (c) epoxy sheet, and (d) epoxy/Dy sheet.

correlation between the prominent Raman intensity at 3068 cm^{-1} and PL intensity variations as a function of UV irradiation time. The linear response of the intensity-induced changes in Raman and PL intensities for the UV-irradiated nanocomposite sheets is visualized in scatter plots in Fig. 8, where the best fit is plotted in red. These include three essential metrics to validate the linear regression model, which were adjusted for the coefficient of determination (R^2), slope of the data distribution, and intercept. The R^2 value provides information about the percentage of the data explained by the linearity of the regression model. In this situation, the slope in the equation represents the magnitude of the change due to UV irradiation; the higher the slope's value, the greater the change. A slope near zero tells us that there is no change. Thus, the slope value can also serve as an indication of the material's sensitivity to UV radiation.

Fig. 8(a) and (b) present the recorded Raman intensities from the epoxy and epoxy/Dy sheets, respectively, as a function of UV irradiation time. A linear fitting based on the variation in irradiation time has been conducted with the data to perform a simple linear regression analysis. The data exhibited an *R*-squared value of 92%, for Raman intensities originating from the neat epoxy sheet. The slopes and intercepts were measured at 2.5 ± 0.3 and 0.7 ± 3.1, respectively. In turn, the sheet of epoxy/Dy presented a value of $R^2 = 98\%$, slope, and intercept of 7.8 ± 0.4 and 10.6 ± 4.1, respectively. It can be observed that the addition of Dy ions to the epoxy matrix increases the values of R^2 and the sensitivity slope. The R^2 also shows that the 1% Dy ions increased the response linearity by 6%. It is also evident from the slope values of the Raman intensity that sensitivity increases. Therefore, in addition to enhancing the linearity of the response, the Dy ions significantly improve the sensitivity of the epoxy sheet to UV radiation.

Fig. 8(c) and (d) give the PL emission intensity change as a function of UV irradiation time for the epoxy and epoxy/Dy sheets, respectively, in a linear mode. PL emission changes were fitted linearly with a simple linear regression model. The PL emissions from the epoxy sheet yielded a semi-linear fit result, with an R^2 of 89%, a slope of 11.0 ± 1.7, and an intercept of 24.1 ± 16.1. Although a linear fit was applied, the observed trend may also be consistent with weak non-linear behavior. In the case of the nanocomposite epoxy/Dy sheet, the R^2 value was 99%, with slope and intercept values of 5.7 ± 0.3 and 7.0 ± 2.9, respectively. A simple linear regression model is used to fit the

PL emissions data from the epoxy sheet, resulting in a poorer fit with an error of 11%. Conversely, the nanocomposite sheet containing Dy ions demonstrated excellent linearity, with an error of only 1%. The PL emission slope from the epoxy sheet was nearly twice that of the Dy-containing sheet, revealing that although the presence of Dy ions improved the linearity of the PL emission data, it decreased the sensitivity of the epoxy sheet to UV light. Therefore, epoxy sheets exhibit better sensitivity to UV radiation, while epoxy/Dy nanocomposite sheets display better linearity.

Sensitivity and linearity are two essential performance parameters in radiation dosimetry. The choice is related to such specific applications, as LiF: Mg, Cu, P, $Li_2B_4O_7$: Mn, and LiF: Mg, Ti are widely used for their tissue–equivalent properties, while $CaSO_4$: Dy, Al_2O_3: C, Mg, Al_2O_3: C, and CaF_2: Mn are selected for their high radiation sensitivity.[47–50] The superior linearity and sensitivity of the Raman and PL emission intensities with UV irradiation indicate the prospective utilization of epoxy and epoxy/Dy nanocomposite sheets in UV radiation dosimetry.

3.5.4 Stability and reproducibility of the PL emission intensities in UV-irradiated sheets. Epoxy and epoxy/Dy nanocomposite sheets were sealed in foil-covered plastic sample bottles to evaluate the stability of the PL emission intensity alterations following UV irradiation. Before capturing the PL emission data, these sheets were left undisturbed for two weeks and one month after irradiation, as illustrated in Fig. 8. In particular, Fig. 9(a) displays the PL emission intensities for the

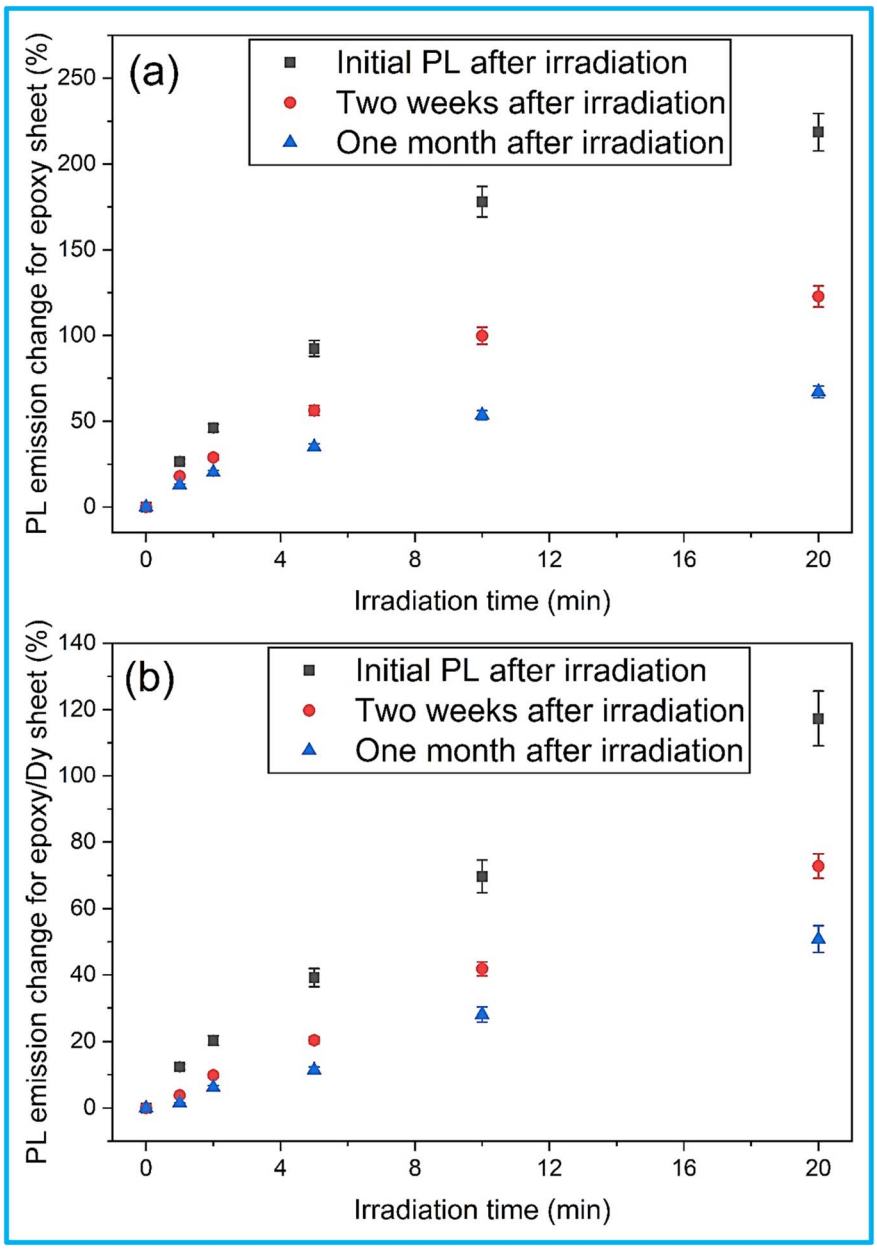

Fig. 9 PL emission intensities stability by comparing initial PL emission intensities and PL emission intensities recorded one month after irradiation: (a) epoxy sheet and (b) epoxy/Dy sheet.

epoxy sheet from the initial reading, as soon as it is exposed to radiation, up to one month. Similarly, the epoxy/Dy nanocomposite sheet is depicted in Fig. 9(b). Interestingly, even after a month of storage, the PL emission intensities from all sheets, including epoxy and epoxy/Dy nanocomposite, retained their linearity, with the data distribution trends indicating little to no change. In contrast, Fig. 9(a) and (b) show a systematic decline in PL emission intensity over time. The PL emission intensity of the epoxy sheet dropped by roughly 71% in a month, but the intensity of the epoxy/Dy nanocomposite sheet dropped by approximately 50%. Despite these significant losses, the Dy ion sheet remained more stable than the epoxy sheet. The PL emission intensity stability of both epoxy and epoxy/Dy nanocomposite sheets decreases after a month of irradiation, indicating that further study is required to improve their stability for practical applications. Nonetheless, the linearity, sensitivity, and repeatability of their signals are promising for further research into UV radiation dosimetry using these nanocomposite sheets.

Infusing Dy ions into the epoxy matrix enhances the linearity of the signal response of the UV-irradiated nanocomposite sheets, providing a consistent and reproducible signal response that highlights their potential in applications requiring precise measurements, such as UV sensing or dosimetry. The slope value in the Raman intensity response indicates that the sheet containing Dy ions is more sensitive to UV radiation than pure epoxy. This implies that epoxy/Dy nanocomposite sheets may detect even small changes induced by UV radiation. Given the above, the good linearity and sensitivity observed in both Raman and PL emission intensities in the nanocomposite sheets containing Dy ions are encouraging for potential UV dosimetry applications. These nanocomposite sheets may provide precise and reliable measurements, which are crucial for controlling and tracking UV exposure in various applications, including industries, medicine, and environmental monitoring. Despite a systematically decreased response, the persistence of PL emission intensities over time in epoxy materials doped with Dy indicates that they retain their linear response after a certain period. While the ability of the devices to remain at equilibrium for at least 3 days is encouraging for potential long-term applications, further efforts are required to minimize the decay of intensity over time. Therefore, the presence of Dy^{3+} ions in the epoxy matrix contributes to the durability of the epoxy's UV response, making it appropriate for long-term practical use.

Moreover, modifying the characteristics of epoxy materials through Dy incorporation offers a wide range of potential applications for Dy-doped epoxy materials. For instance, highly sensitive nanocomposites can be developed for detecting low-level UV radiation, while nanocomposite sheets with high linearity can be created for applications requiring precise measurements. Similar to the selection of materials like LiF: Mg, Cu, P for tissue-equivalent characteristics or $CaSO_4$: Dy for high sensitivity, this customization fits the needs of various dosimetric applications where varying degrees of sensitivity and accuracy are required.[47,49] The results emphasize the necessity for more investigation to maximize PL emission intensity stability over long timeframes. This is because the enhancement of the stability of epoxy nanocomposite sheets under UV irradiation will enhance their potential real applications and vulnerability. Thus, doped Dy ions in the epoxy matrices not only improve the linearity and sensitivity of the epoxy sheet's response to UV radiation but also pave new avenues for their application in radiation dosimetry and in several other applications where precise and reproducible detection of radiation is a prerequisite.

4. Conclusions

This study investigates the effects of Dy^{3+} ion addition into the epoxy matrix in the form of nanocomposite sheets on their structural and optical properties, as well as the impact of UV irradiation. The fabricated nanocomposite sheets were studied using various techniques, including SEM, XRD, Raman spectroscopy, and photoluminescence (PL). The epoxy sheet containing Dy^{3+} ions exhibited an almost uniform distribution of nanoparticles, with nanoparticle sizes decreasing slightly with increasing Dy concentration. Changes were observed in the Raman spectra, particularly in the intensities and FWHM. These changes were attributed to the possible formation of defects in the chemical structure, including the crystalline structure, as confirmed by the changes observed in the average crystallite size. The variation of Dy concentrations also affects the PL emission intensities by narrowing the PL spectra, increasing the PL intensities, and shifting the center position of the PL spectrum. This narrowing reflection suggests the development of defects or carrier transfer within the epoxy matrix, resulting in increased PL intensities. The observed shift in the PL emission peak position indicates tuning of light emission; it may also be related to the changes in surface morphology resulting from partial interaction between Dy^{3+} ions and epoxy, as shown in the SEM images. The nanocomposite sheets were later exposed to UV radiation at different times. The irradiation causes changes in the Raman and PL emission intensities, which are attributed to the UV light-induced changes in the chemical bonds and possible degradation. The pure and epoxy/Dy nanocomposite sheets showed excellent linear UV response and sensitivity to UV exposure. However, the epoxy/Dy nanocomposite sheet showed superior stability. Hence, incorporating Dy^{3+} ions into the epoxy matrix enhances the linearity of the response and stability under UV exposure, suggesting their potential use in UV radiation sensing and/or radiation dosimetry, as well as other applications requiring consistent and reliable UV detection.

Data availability

All underlying data are available in the article itself and its ESI.†

Author contributions

Shittu Abdullahi: conceptualization, investigation, methodology, data curation, formal analysis, writing – original draft. Ahmed Alshahrie: resources, writing – reviewing and editing.

Aznan Fazli Ismail: writing – reviewing and editing, resources. Numan Salah: supervision, validation, writing – review & editing, funding acquisition, resources.

Conflicts of interest

The authors declare that they have no known competing financial interests or personal relationships that could have appeared to influence the work reported in this paper.

Acknowledgements

This scientific paper is derived from a research grant funded by the Research, Development, and Innovation Authority (RDIA) – Kingdom of Saudi Arabia – with grant number (12965-kau-2023-KAU-R-3-1-SE-).

Notes and references

1 X. Tao, M. Wei, X. Hu, Y. Tang, W. Wei, J. Liu and X. Li, *Polymer*, 2024, **302**, 127093.
2 C. D. Varganici, L. Rosu, D. Rosu, I. Rosca, M. E. Ignat and L. Ignat, *Polymers*, 2024, **16**, 67.
3 N. A. Mohammad, S. H. Ahmad, R. S. Chen and N. E. N. A. Mohammad, *J. Appl. Polym. Sci.*, 2021, **139**, e51812.
4 Z. F. Merzah, S. Fakhry, T. G. Allami, N. Y. Yuhana and A. Alamiery, *Polymers*, 2022, **14**, 526.
5 C. D. Varganici, L. Rosu, S. Lehner, C. Hamciuc, M. Jovic, D. Rosu, F. Mustata and S. Gaan, *Mater. Des.*, 2021, **212**, 110237.
6 M. Zhao, L. Meng, L. Ma, L. Ma, X. Yang, Y. Huang, J. E. Ryu, A. Shankar, T. Li, C. Yan and Z. Guo, *Compos. Sci. Technol.*, 2018, **154**, 28–36.
7 T. Q. Liu, X. Liu and P. Feng, *Composites, Part B*, 2020, 107958, DOI: 10.1016/j.compositesb.2020.107958.
8 C. Wu, B. C. Meng, L. Ho Tam and L. He, *Polym. Test.*, 2022, **114**, 107708.
9 X. Wan, B. Demir, M. An, T. R. Walsh and N. Yang, *Int. J. Heat Mass Transf.*, 2021, **180**, 121821.
10 W. L. Hsu, C. C. Liu, Y. C. Shiau and W. C. Lin, *Sustainability*, 2019, **11**, 1756.
11 K. Nehra, A. Dalal, A. Hooda, S. Bhagwan, R. K. Saini, B. Mari, S. Kumar and D. Singh, *J. Mol. Struct.*, 2022, **1249**, 131531.
12 E. M. Goldys, K. Drozdowicz-Tomsia, S. Jinjun, D. Dosev, I. M. Kennedy, S. Yatsunenko and M. Godlewski, *J. Am. Chem. Soc.*, 2006, **128**, 14498–14505.
13 B. S. Panigrahi, *Spectrochim. Acta, Part A*, 2000, **56**, 1337–1344.
14 A. A. Knyazev, A. S. Krupin and Y. G. Galyametdinov, *J. Lumin.*, 2022, **242**, 118609.
15 C. G. Gameiro, S. Alves, E. F. Da Silva, C. A. Achete, R. A. Simão and P. A. Santa-Cruz, in *Materials Characterization*, Elsevier Inc., 2003, vol. 50, pp. 109–116.
16 W. G. Quirino, C. Legnani, M. Cremona, P. P. Lima, S. A. Junior and O. L. Malta, in *Thin Solid Films*, 2006, vol. 494, pp. 23–27.
17 P. K. Shahi, A. K. Singh, S. B. Rai and B. Ullrich, *Sens. Actuators, A*, 2015, **222**, 255–261.
18 J. Yu, L. Zhou, H. Zhang, Y. Zheng, H. Li, R. Deng, Z. Peng and Z. Li, *Inorg. Chem.*, 2005, **44**, 1611–1618.
19 A. M. Kaczmarek, *J. Mater. Chem. C*, 2018, **6**, 5916–5925.
20 S. Khursheed, A. S. Sheergojri and J. Sharma, in *Materials Today: Proceedings*, 2020, vol. 21, pp. 2096–2104.
21 V. Prajzler, V. Jerabek, I. Huttel, O. Lyutakov, J. Spirkova, V. Machovic, J. Oswald and J. Zavadil, in *Novel Optical Systems Design and Optimization XI*, SPIE, 2008, vol. 7061, p. 706119.
22 E. Yousif and R. Haddad, *Springerplus*, 2013, **2**, 398.
23 G. M. Odegard and A. Bandyopadhyay, *J. Polym. Sci. B*, 2011, **49**, 1695–1716.
24 S. Chong, B. J. Riley, J. Marcial, C. E. Lonergan and D. A. Cutforth, *J. Chem. Crystallogr.*, 2022, **52**, 185–193.
25 K. Gopinath, M. Chinnadurai, N. P. Devi, K. Bhakyaraj, S. Kumaraguru, T. Baranisri, A. Sudha, M. Zeeshan, A. Arumugam, M. Govindarajan, N. S. Alharbi, S. Kadaikunnan and G. Benelli, *J. Cluster Sci.*, 2017, **28**, 621–635.
26 B. J. Jaques and D. P. Butt, *J. Alloys Compd.*, 2015, **644**, 211–222.
27 N. D. Sharma, J. Singh, S. Dogra, D. Varandani, H. K. Poswal, S. M. Sharma and A. K. Bandyopadhyay, *J. Raman Spectrosc.*, 2011, **42**, 438–444.
28 X. Liao, F. Peng, Y. Pu, S. Cao and D. Zhu, *J. Electron. Mater.*, 2021, **50**, 1963–1979.
29 M. Irfan and A. Shakoor, *J. Inorg. Organomet. Polym. Mater.*, 2020, **30**, 1287–1292.
30 M. M. Kaid, A. S. Khder, S. A. Ahmed, A. A. Ibrahim, H. M. Altass, R. I. Alsantali, R. S. Jassas, M. A. Khder, M. M. Al-Rooqi, Z. Moussa and A. I. Ahmed, *ACS Omega*, 2022, **7**, 17223–17233.
31 V. Olifirenko, A. Abduraimova, M. S. Kang, I. S. Raja, B. Duisenbayeva, A. Molkenova, L. Khamkhash, Y. H. Hwang, D. W. Han and T. S. Atabaev, *Nano Express*, 2021, **2**, 010022.
32 O. P. Moreno, M. C. Portillo, H. J. Santiesteban, J. A. Pulidoc, Y. R. Reynoso and L. S. de la Rosa, *Rev. Mex. Fis.*, 2023, **69**, 1–12.
33 Z. Heng, Y. Chen, H. Zou and M. Liang, in *Handbook of Epoxy Blends*, ed. J. Parameswaranpillai, N. Hameed, J. Pionteck and E. M. Woo, Springer, 2017, pp. 147–184.
34 S. Nikafshar, O. Zabihi, S. Hamidi, Y. Moradi, S. Barzegar, M. Ahmadi and M. Naebe, *RSC Adv.*, 2017, **7**, 8694–8701.
35 A. Saeed, E. Banoqitah, A. Alaqab, A. Alshahrie, M. A. Saleh, A. M. Alhawsawi, M. M. Damoom and N. Salah, *ACS Omega*, 2022, **8**, 747–760.
36 N. M. Yussuf, A. F. Ismail, N. A. Mohamed and M. A. Mat Teridi, *Mater. Lett.*, 2024, **357**, 135771.
37 A. F. Betancur, A. García and F. R. Pérez, *J. Phys. Conf. Ser.*, 2019, **1219**, 012003.

38 S. Abdullahi, Y. N. Salah, A. Alshahrie and N. Salah, *Radiat. Phys. Chem.*, 2025, **226**, 112259.
39 S. Abdullahi, A. F. Ismail, A. Alshahrie, M. M. Damoom, E. Banoqitah and N. Salah, *Radiat. Phys. Chem.*, 2025, **236**, 112907.
40 I. N. Nawas Mumthas, M. F. Mohamad Noh, N. A. Arzaee, N. A. Mohamed, S. N. F. Mohd Nasir, H. Alessa, A. F. Ismail, H. Moria and M. A. Mat Teridi, *Int. J. Energy Res.*, 2021, **45**, 15284–15297.
41 S. V. Koniakhin, O. I. Utesov and A. G. Yashenkin, *Diamond Relat. Mater.*, 2024, **146**, 111182.
42 A. Baillard, P.-A. Douissard, P. Loiko, T. Martin, E. Mathieu and P. Camy, *RSC Adv.*, 2025, **15**, 18802.
43 S. Abdullahi, A. Alshahrie, E. Banoqitah, S. M. U. G. Mohiuddin and N. Salah, *Radiat. Phys. Chem.*, 2023, **206**, 110775.
44 S. Abdullahi, A. Alshahrie, E. Banoqitah, M. M. Damoom and N. Salah, *J. Lumin.*, 2023, **257**, 119696.
45 S. Sanguinetti, M. Henini, M. G. Alessi, M. Capizzi, P. Frigeri and S. Franchi, *Phys. Rev. B: Condens. Matter Mater. Phys.*, 1999, **60**, 8276–8283.
46 X. Su, Z. Zhang and M. Zhu, *Appl. Phys. Lett.*, 2006, **88**, 061913.
47 IAEA, *Dosimetry in Diagnostic Radiology: An International Code of Practice (Technical Reports Series No. 457)*, Vienna, 2007.
48 S. Abdullahi, A. Aydarous and N. Salah, *Radiat. Phys. Chem.*, 2021, **188**, 109656.
49 IAEA, *Radiation Oncology Physics: A Handbook for Teachers and Students*, International Atomic Energy Agency, Vienna, 2005.
50 S. Abdullahi, A. Aydarous and N. Salah, *J. Lumin.*, 2022, **242**, 118588.